

Detection and characterization of microseismic sources with shaped DAS fibre

Kris Innanen, Faranak Mahmoudian and Matthew Eaid

ABSTRACT

A significant possible application of fibre-optic DAS sensing, assuming it becomes robustly sensitive to a range of different strain components, is for the characterization of microseismic sources. In this paper we adjust the growing DAS geometrical model (the CREWES FGSM) such that it can be brought to bear on the problem of sensing various moment tensors. The model is so designed that the *appraisal problem* (i.e.: “for a source at the following position with the following focal mechanism, can the moment tensor be resolved by the given fibre shape and fibre parameters?”) is straightforward. It is hoped that this line of inquiry will dovetail with the microseismic FWI work reported this year.

INTRODUCTION

In this short note we merge results begun in 2016 and continued in 2017 to pose the moment tensor / focal mechanism inversion problem, either directly (Mahmoudian and Innanen, 2016), or in the context of full waveform inversion and assuming an imperfectly known velocity model (Igonin and Innanen, 2017a,b), and to enable important monitoring with the acquisition technology known as Distributed Acoustic Sensing (DAS). Full referencing and model description for the latter can be found in the reports by Innanen (2016); Innanen and Eaid (2017).

The set up is as follows. In the next section we select a simple surface configuration of both straight and helical-wound cable (HWC) DAS. In the following section we set out the quantities needed to accept an input source moment tensor, elastic P- and S-wave velocities, and propagate those source signatures into the DAS fibre, determining its response. This represents a simple and computable model for appraisal of fibre shape design as a means to detect and locate sources, and distinguish and ultimately invert for focal mechanisms.

STRAIGHT AND HELICAL-WOUND SURFACE FIBRE ARRAYS

We create two benchmark fibre surface acquisition “arrays” upon which to exemplify the focal mechanism / shaped fibre response modelling. A set of parallel fibre lines in the x_2 direction are connected by semi-circular arcs to form a repeating S-shape pattern. In the right panel of Figure 1 this shape is illustrated at the surface of a rectangular volume, 0.3km by 0.3km laterally and 0.18km vertically; in the left panel the corresponding HWC is illustrated (helix radius exaggerated for illustration purposes).

FAR-FIELD ELASTIC STRAINS INDUCED BY MICROSEISMIC SOURCES

We will assume a simple (homogeneous) isotropic-elastic medium, within which a source at position $\mathbf{x}_s = (x_1^s, x_2^s, x_3^s)^T$ is set off, radiating with a moment tensor \mathbf{M} upward towards a surface, just below which a DAS fibre with a given geometry/shape senses the longitudinal strain (or strain-rate) in the axial direction of the fibre.

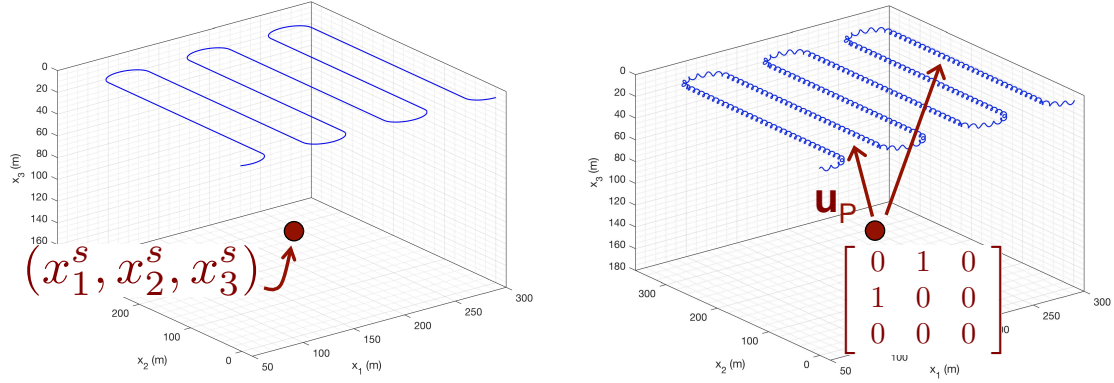


FIG. 1. Left panel: a sequence of parallel straight fibre lines, parallel to the x_2 axis are arrayed along the x_1 axis, and joined by semi-circular connectors to form a repeating S-pattern. A source is placed at an arbitrary point in the volume. Right panel: in this case the straight lines are used as the axes of a helix, simulating an HWC laid out in the S-pattern. The focal mechanism of the source determines the P- and S-wave displacements and strains at points along the length of the fibre.

P- and S-wave strain-displacement relations

The displacement $\mathbf{u}(\mathbf{x})$ measured at position \mathbf{x} has P- and S-wave components and is decomposable into

$$\mathbf{u}(\mathbf{x}) = u_i = \mathbf{u}_P(\mathbf{x}) + \mathbf{u}_S(\mathbf{x}). \quad (1)$$

In a Cartesian system (inline x_1 , crossline x_2 , and depth x_3), the observation position has components

$$\mathbf{x} = \begin{bmatrix} x_1 \\ x_2 \\ x_3 \end{bmatrix}. \quad (2)$$

In order to keep both vector and indicial notation available at all times (either may be more useful at almost any time), we write

$$\begin{aligned} \mathbf{u}_P(\mathbf{x}) &= u_i^P \\ \mathbf{u}_S(\mathbf{x}) &= u_i^S. \end{aligned} \quad (3)$$

Similarly we will assume the strain associated with these displacements can be decomposed into that carried by P-waves and that carried by S-waves:

$$\mathbf{e}(\mathbf{x}, t) = e_{ij} = \mathbf{e}^P(\mathbf{x}, t) + \mathbf{e}^S(\mathbf{x}, t), \quad (4)$$

where

$$\begin{aligned} \mathbf{e}^P(\mathbf{x}, t) &= e_{ij}^P \\ \mathbf{e}^S(\mathbf{x}, t) &= e_{ij}^S. \end{aligned} \quad (5)$$

The relationship between general strain and general displacement is linear:

$$\begin{aligned} e_{ij} &= \frac{1}{2} \left[\frac{\partial u_i}{\partial x_j} + \frac{\partial u_j}{\partial x_i} \right] \\ &= \frac{1}{2} \left[\frac{\partial u_i^P}{\partial x_j} + \frac{\partial u_j^P}{\partial x_i} \right] + \frac{1}{2} \left[\frac{\partial u_i^S}{\partial x_j} + \frac{\partial u_j^S}{\partial x_i} \right], \end{aligned} \quad (6)$$

in which case the standard formula for transforming displacement to strain can be applied to the decomposition

$$\begin{aligned} e_{ij}^P &= \frac{1}{2} \left[\frac{\partial u_i^P}{\partial x_j} + \frac{\partial u_j^P}{\partial x_i} \right], \\ e_{ij}^S &= \frac{1}{2} \left[\frac{\partial u_i^S}{\partial x_j} + \frac{\partial u_j^S}{\partial x_i} \right]. \end{aligned} \quad (7)$$

Next we will follow Mahmoudian and Innanen (2016), adopting expressions for the displacement caused by seismic sources as quoted by Aki and Richards (2002), and use the above formulas to transform to strain, and thence to the fibre response.

Far-field displacements from general seismic sources

If a source is set off and observed at a positions

$$\begin{bmatrix} x_1^s \\ x_2^s \\ x_3^s \end{bmatrix} \quad \text{and} \quad \begin{bmatrix} x_1^g \\ x_2^g \\ x_3^g \end{bmatrix}, \quad (8)$$

and times t_s and t_g , respectively, the expressions in the previous section, with t meaning $t_g - t_s$, and \mathbf{x} meaning $\mathbf{x}_g - \mathbf{x}_s$, can be used to quantify observations of strain and displacement caused by the source. Temporarily neglecting time-variations, let us assume that the source induces mechanical waves via the moment tensor, which has the form

$$\mathbf{M} = M_{ij} = \begin{bmatrix} M_{11} & M_{12} & M_{13} \\ M_{21} & M_{22} & M_{23} \\ M_{31} & M_{32} & M_{33} \end{bmatrix}, \quad (9)$$

when resolved in the inline-crossline-depth coordinate system. What are the P- and S-wave displacements observed at \mathbf{x} and t ? For convenience we define the vector

$$\mathbf{g} = \gamma_i = \begin{bmatrix} \gamma_1 \\ \gamma_2 \\ \gamma_3 \end{bmatrix}, \quad (10)$$

such that the elements are the direction cosines

$$\gamma_1 = \frac{x_1}{r}, \quad \gamma_2 = \frac{x_2}{r}, \quad \gamma_3 = \frac{x_3}{r}, \quad (11)$$

where

$$r = (\mathbf{x}^T \mathbf{x})^{1/2} = (x_1^2 + x_2^2 + x_3^2)^{1/2}. \quad (12)$$

Defining the useful scalar and tensor quantities

$$m = \mathbf{g}^T \mathbf{M} \mathbf{g}, \quad (13)$$

and

$$\mathbf{D} = D_{ij} = \mathbf{I} - \mathbf{g} \mathbf{g}^T = \delta_{ij} - \gamma_i \gamma_j, \quad (14)$$

the components of displacement at \mathbf{x} are given by (Aki and Richards, 2002)

$$\begin{aligned} u_i^P &= \mathbf{u}_P = \left(\frac{c_\alpha}{r}\right) m \mathbf{g} = \left(\frac{c_\alpha}{r}\right) m \gamma_i, \\ u_i^S &= \mathbf{u}_S = \left(\frac{c_\beta}{r}\right) (\mathbf{M} \mathbf{g} - m \mathbf{g}) = \left(\frac{c_\alpha}{r}\right) (M_{ij} \gamma_j - m \gamma_i), \end{aligned} \quad (15)$$

where

$$c_\alpha = (4\pi\rho\alpha^2)^{-1}, \quad \text{and} \quad c_\beta = (4\pi\rho\beta^2)^{-1}. \quad (16)$$

These displacements have associated strains, which we will compute next.

Far-field strains

In order to discuss strain response, the next thing that is needed is the strain tensor, evaluated in the inline-crossline-depth coordinate system, associated with the displacements in equation (15). To this end, several more convenient quantities are introduced:

$$\frac{\partial}{\partial x_j} \left(\frac{1}{r}\right) = -\left(\frac{1}{r^2}\right) \gamma_j = -\left(\frac{1}{r^2}\right) \mathbf{g}, \quad (17)$$

and

$$\frac{\partial \gamma_i}{\partial x_j} = \left(\frac{1}{r}\right) D_{ij} = \left(\frac{1}{r}\right) \mathbf{D}, \quad (18)$$

and finally

$$\begin{aligned} \frac{\partial m}{\partial x_j} &= \left(\frac{1}{r}\right) (D_{pj} M_{pq} \gamma_q + \gamma_p M_{pq} D_{qj}) \\ &= \left(\frac{1}{r}\right) (\mathbf{D}^T \mathbf{M} \mathbf{g} + \mathbf{g}^T \mathbf{M} \mathbf{D}). \end{aligned} \quad (19)$$

The formulas in equation (8), applied to the displacements in equations (15), lead to strain responses

$$e_{ij}^P = \frac{c_\alpha}{r^2} \left[\gamma_i \left(D_{pj} M_{pq} \gamma_q + \gamma_p M_{pq} D_{qj} \right) - m \gamma_i \gamma_j + m D_{ij} \right], \quad (20)$$

or

$$\mathbf{e}^P = \frac{c_\alpha}{r^2} \left[\mathbf{g} \left(\mathbf{D}^T \mathbf{M} \mathbf{g} + \mathbf{g}^T \mathbf{M} \mathbf{D} \right)^T - m \mathbf{g} \mathbf{g}^T + m \mathbf{D} \right], \quad (21)$$

for the P-wave component, and

$$e_{ij}^S = \frac{c_\beta}{r^2} \left[M_{iq} D_{qj} - \gamma_j M_{iq} \gamma_q + m \gamma_i \gamma_j - \gamma_i \left(D_{pj} M_{pq} \gamma_q + \gamma_p M_{pq} D_{qj} \right) - m D_{ij} \right], \quad (22)$$

or

$$\mathbf{e}^S = \frac{c_\beta}{r^2} \left[\mathbf{M} \mathbf{D} - \mathbf{g} (\mathbf{M} \mathbf{g})^T + m \mathbf{g} \mathbf{g}^T - \mathbf{g} \left(\mathbf{D}^T \mathbf{M} \mathbf{g} + \mathbf{g}^T \mathbf{M} \mathbf{D} \right)^T - m \mathbf{D} \right], \quad (23)$$

for the S-wave component.

Propagation and time delay

The displacements \mathbf{u}_P and \mathbf{u}_S are carried from the source to the observation points at speeds α and β respectively:

$$\begin{aligned} \mathbf{u}_P(\mathbf{x}, t) &= \mathbf{u}_P(\mathbf{x}) \dot{s} \left(t - \frac{r}{\alpha} \right), \\ \mathbf{u}_S(\mathbf{x}, t) &= \mathbf{u}_S(\mathbf{x}) \dot{s} \left(t - \frac{r}{\beta} \right). \end{aligned} \quad (24)$$

If we take this same picture, in which time variations of the response are produced by allowing the space variations (i.e., the moment tensor directionality, “spread out” over a ball of radius r), to be scaled and time-delayed, and apply it to the strain, we obtain

$$\begin{aligned} \mathbf{e}^P(\mathbf{x}, t) &= \mathbf{e}^P(\mathbf{x}) \dot{s} \left(t - \frac{r}{\alpha} \right), \\ \mathbf{e}^S(\mathbf{x}, t) &= \mathbf{e}_S^S(\mathbf{x}) \dot{s} \left(t - \frac{r}{\beta} \right). \end{aligned} \quad (25)$$

This is *wrong*, because the derivatives in the transformation from displacement to strain should have been applied to the r/α and r/β terms. The strain is sensitive to changes in displacement across differential distances in space. The terms that are missing, if we use equations (25), account for the fact that displacement information is arriving at these differentially separated spatial points at different times. For sufficiently low frequency wavelets this should be a small effect, so we will admit this source of error in order to keep the relatively simple formulas we are currently working with.

MODELING DAS FIBRE RESPONSE

Any point along a DAS fibre can now be assigned a time-varying strain tensor in the inline-crossline-depth coordinate system. The CREWES FGSM model (Innanen and Eaid, 2017) is set up to receive this information, create the geometrical quantities needed to

characterize the fibre shape at all points along its length, and determine the response. This will amount to rotating the strain into the local coordinate system of the fibre and extracting the longitudinal/axial component (which we have been calling e_{tt}).

As test source mechanisms, we choose

$$\mathbf{M}_1 = \begin{bmatrix} 0 & 1 & 0 \\ 1 & 0 & 0 \\ 0 & 0 & 0 \end{bmatrix}, \quad \mathbf{M}_2 = \begin{bmatrix} 1 & 0 & 0 \\ 0 & 0 & 0 \\ 0 & 0 & 0 \end{bmatrix}, \quad (26)$$

and examine their variable response in the fibre.

Arc-length map of the (time-invariant) maximum strain response

The time-invariant quantities $e^P(\mathbf{x})$ and $e^S(\mathbf{x})$ arrive at the point \mathbf{x} (e.g., a point along the fibre) at *some point in time*, dictated by the scaling in the function s and the velocities α and β . If s is normalized such that the maximum of \dot{s} is 1, then every point \mathbf{x} along the fibre will, eventually, experience $e^P(\mathbf{x})$ and $e^S(\mathbf{x})$. A map of either of these, the maximum fibre response at all points along its arc-length to either the P-mode or the S-mode, is a quick and very informative quantification of the fibre shape and the moment tensor being examined. The sum is not particularly useful, as the two modes would never arrive simultaneously.

In Figure 2 the maximum strain responses for the P-components produced by moment tensors \mathbf{M}_1 and \mathbf{M}_2 are plotted for both the straight (top panel) and HWC (bottom panel) fibres.

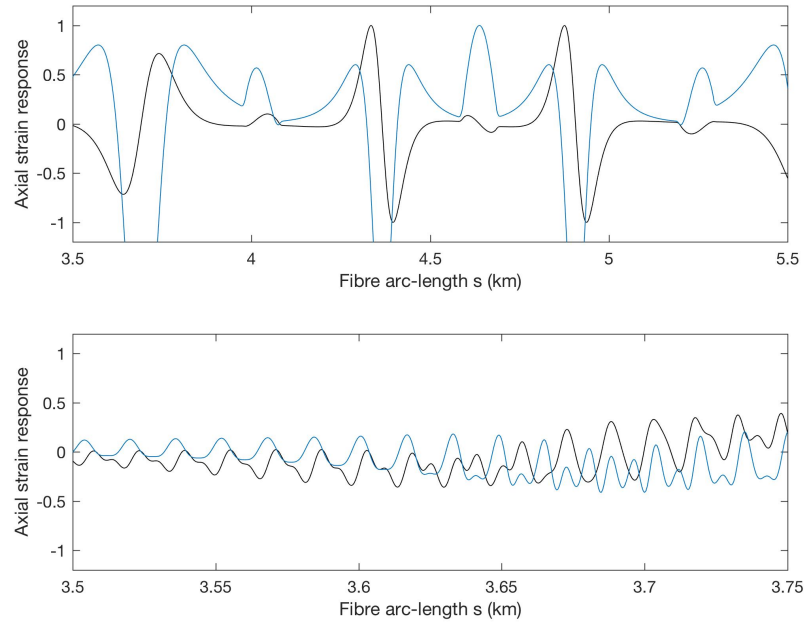


FIG. 2. Top panel: maximum P-wave strains produced by moment tensors \mathbf{M}_1 (blue) and \mathbf{M}_2 (black) for the straight fibre. Bottom panel: maximum P-wave strains produced by moment tensors \mathbf{M}_1 (blue) and \mathbf{M}_2 (black) for the HWC fibre. Note the difference in the horizontal axis limits.

Time-variant arc-length response: microseismic shot records

Choosing as the source wavelet the first derivative of a Gaussian, \dot{s} takes the form of a Ricker wavelet. The P-wave component is given a dominant frequency of 30Hz and the S-wave a dominant frequency of 15Hz; the P-wave velocity in the medium is set at 2.0km/s and the S-wave velocity at 1.0km/s.

The shot record is calculated with $t = 0$ set at the moment of the first arriving P-energy. In Figure 3a the record for moment tensor M_1 is plotted; in Figure 3b the record for moment tensor M_2 is plotted.

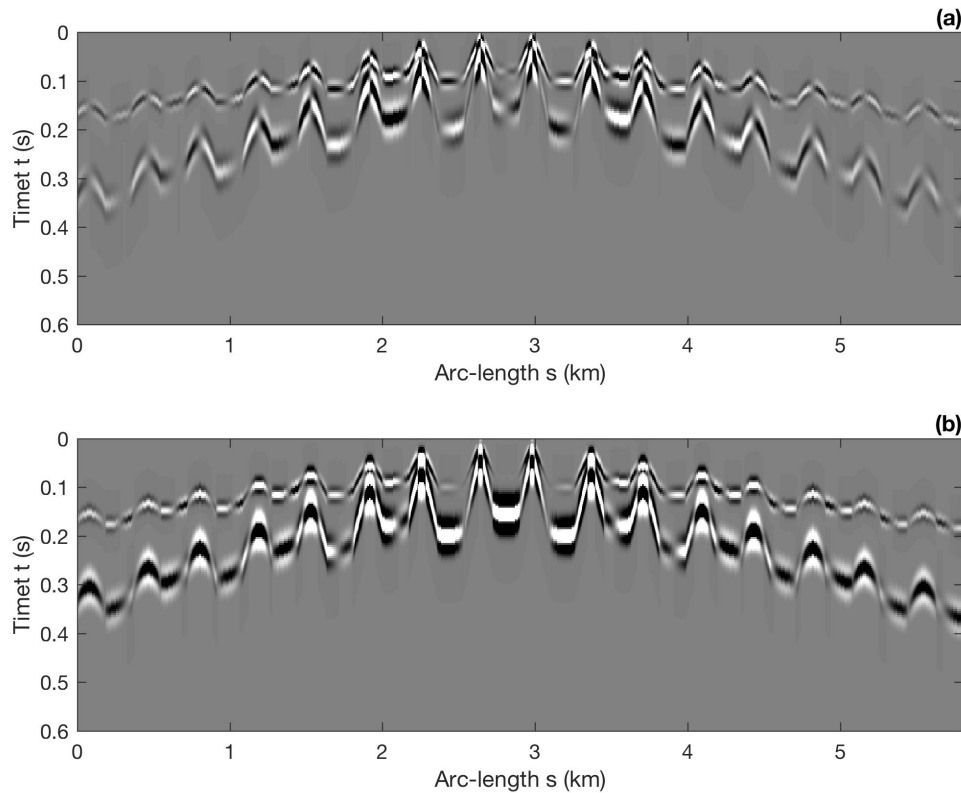


FIG. 3. (a) Full fibre response to the P- and S-waves propagating from a source at (b)

CONCLUSIONS

In 2016 Mahmoudian and Innanen explored the features of the moment tensor inverse problem; in 2017 Igonin began to frame the FWI problem for determining source characteristics in the absence of an accuracy velocity model. Here we tie the microseismic source problem to our growing model of DAS fibre response. This report describes a way-point as we bring all of these techniques and technologies together.

ACKNOWLEDGEMENTS

We thank the sponsors of CREWES for continued support. This work was funded by CREWES industrial sponsors and NSERC (Natural Science and Engineering Research Council of Canada) through the grant CRDPJ 461179-13.

REFERENCES

- Aki, K., and Richards, P. G., 2002, *Quantitative Seismology*: University Science Books, 2nd edn.
- Igonin, N., and Innanen, K. A., 2017a, Applications of FWI to the microseismic source problem: CREWES Annual Report, **29**.
- Igonin, N., and Innanen, K. A., 2017b, Toward full-waveform inversion for source location and velocity model: gradient and Hessian: CREWES Annual Report, **29**.
- Innanen, K. A., 2016, A geometrical model of DAS fibre response: CREWES Annual Report, **28**.
- Innanen, K. A., and Eaid, M., 2017, Design of DAS fibres for elastic wave mode discrimination: CREWES Annual Report, **29**.
- Mahmoudian, F., and Innanen, K. A., 2016, Towards seismic moment tensor inversion for source mechanisms: CREWES Annual Report, **28**.